

**CHITOSAN-BENTONITE COMPOSITE FOR THE REMOVAL OF  
TARTRAZINE, MALACHITE GREEN AND COPPER (II) FROM AQUEOUS  
SOLUTION**

**by**

**NOORUL FARHANA BINTI MD ARIFF**

**Thesis submitted in fulfilment of the  
requirements for the degree  
of Master of Science**

**January 2011**



## **ACKNOWLEDGEMENTS**

Alhamdulillah. I am so grateful to Allah SWT for giving me this opportunity for completing my study, giving me good health and good people around me during my study.

I would like to express million of thanks to my supervisor Assoc. Prof. Dr. Wan Saime Wan Ngah for guiding me either in my labwork, writing papers and this thesis. I am really appreciate his support and guides. Thank you also for my family especially my parents, Dr. Md Ariff Abas and Mrs. Wan Sepiah Shiekh Ibrahim and my fiance, Mr. Mohd. Tarmizi Zakaria for encouraging me in this study.

This study will not be successful without the participation of these persons: Tuan Hj. Arifin Majid, Mrs. Norhayati Abdul Kadir, Mr. Marimuthu Ayeroo, Mr. Aw Yeong Choek Hoe, and Mr Ong Ching Hin. Not forgetable my labmates; Dr. Megat Ahmad Kamal Megat Hanafiah and Dr. Sharon Fatinathan for guiding, helping and supporting me, my friends; Ms. Nur Syazwani Mohd Yusoff, Ms. Sharifah Athirah Abas, Ms. Waheeba Ahmed, Ms. Affaizza Mohd Shah, Ms. Rozaini Che Amat and Mrs. Roslinda Ali.

Last but not least, Pusat Pengajian Sains Kimia, Institut Pengajian Siswazah and Universiti Sains Malaysia, Pulau Pinang.

## TABLE OF CONTENTS

	Page
Acknowledgements	ii
Table of Content	iii
List of Tables	viii
List of Figures	x
List of Abbreviations and Symbols	xiv
Abstrak	xvii
Abstract	xix

### CHAPTER ONE: INTRODUCTION

1.1	Water Pollution	1
1.2	Dyes	2
	1.2.1 Tartrazine	3
	1.2.2 Malachite Green	5
1.3	Heavy Metal Ion	7
	1.3.1 Copper	8
1.4	Chitin and Chitosan	11
1.5	Bentonite	14
1.6	Modifications of Chitosan	15
1.7	Chitosan Composite	
	1.7.1 Chitosan-Alumina/Silica Composite	18
	1.7.2 Chitosan-Montmorillonite Composite	19
	1.7.3 Chitosan-Perlite Composite	20
	1.7.4 Chitosan-Fe <sub>3</sub> O <sub>4</sub> Composite	21
	1.7.5 Chitosan-Activated Carbon Composite	22
1.8	Adsorption	22
	1.8.1 Adsorption Kinetic	24

1.8.2	Adsorption Isotherm	25
1.8.3	Temperature Variation	27
1.9	Research Objectives	28

## **CHAPTER TWO: EXPERIMENTAL**

2.1	Chemicals and Instruments Used for the Research	
2.1.1	List of Chemicals	30
2.1.2	List of Instruments	31
2.2	Determination of Degree of Deacetylation	32
2.3	Preparation of Chitosan and Composite Chitosan-Bentonite (CCB) Beads	
2.3.1	Preparation of Chitosan Beads	33
2.3.2	Preparation of CCB Beads	34
2.4	Characterizations of CCB Beads	
2.4.1	Solubility Test	35
2.4.2	Swelling Test	35
2.4.3	$\text{pH}_{\text{slurry}}$ and $\text{pH}_{\text{ZPC}}$	36
2.4.4	The Fourier Transform Infrared Spectroscopy (FTIR)	36
2.4.5	Scanning Electron Microscopy (SEM)	37
2.4.6	Determination of Average Pore Diameter and Surface Area	37
2.4.7	X-Ray Diffraction (XRD)	37
2.5	UV-Visible Spectroscopy and Atomic Absorption Spectroscopy Analysis	38
2.6	Preparation of Stock Solution for Tartrazine, MG and Copper (II) Ion	
2.6.1	Preparation of $250 \text{ mg L}^{-1}$ of Tartrazine Stock Solution	38
2.6.2	Preparation of $250 \text{ mg L}^{-1}$ of MG Stock Solution	38
2.6.3	Preparation of $1000 \text{ mg L}^{-1}$ of Copper (II) Ion Stock Solution	39

2.7	Standard Calibration Curve for Tartrazine, MG and Copper (II) Ion	39
2.7.1	Standard Calibration Curve for Tartrazine	40
2.7.2	Standard Calibration Curve for MG	40
2.7.3	Standard Calibration Curve for Copper (II) Ion	41
2.8	Batch adsorption studies	41
2.8.1	Determination of Precipitation pH of Copper Hydroxide	42
2.8.2	Effect of pH for Adsorption of Tartrazine, MG and Copper (II) Ion onto CCB Beads	43
2.8.3	Effect of Stirring Speed for Adsorption of Tartrazine, MG and Copper (II) Ion onto CCB Beads	44
2.8.4	Effect of Adsorbent Dosage for Adsorption of Tartrazine, MG and Copper (II) Ion onto CCB Beads	45
2.8.5	Effect of Concentration and Contact Time for Adsorption of Tartrazine, MG and Copper (II) Ion onto CCB Beads	46
2.8.6	Adsorption Isotherm and Temperature Variation	47
2.9	Desorption Study	48

### **CHAPTER THREE: RESULTS AND DISCUSSIONS**

3.1	Deacetylation Degree	50
3.2	Characterization of CCB beads	51
3.2.1	Solubility Test	51
3.2.2	Swelling Test	52
3.2.3	pH <sub>slurry</sub> and pH <sub>ZPC</sub>	53
3.2.4	The Fourier Transform Infrared Spectroscopy (FTIR)	54
3.2.5	Scanning Electron Microscopy (SEM)	56
3.2.6	Determination of Average Pore Diameter and Surface Area	57
3.2.7	X-Ray Diffraction (XRD)	59

3.2.8	Proposed Mechanism for Preparation of CCB Beads	60
3.3	Batch adsorption study	
3.3.1	Determination of Precipitation pH of Copper Hydroxide	62
3.3.2	Effect of Initial pH for Adsorption of Tartrazine, MG and Copper (II) Ion onto CCB Beads	63
3.3.3	Effect of Stirring Speed for Adsorption of Tartrazine, MG and Copper (II) Ion onto CCB beads	67
3.3.4	Effect of Adsorbent Dosage for Adsorption of Tartrazine, MG and Copper (II) Ion onto CCB beads	69
3.3.5	Effect of Initial Concentration and Stirring Time for Adsorption of Tartrazine, MG and Copper (II) Ion onto CCB Beads	72
3.4	Adsorption Kinetic	77
3.4.1	Pseudo-first-order Kinetic Model	78
3.4.2	Pseudo-second-order Kinetic Model	82
3.4.3	Intraparticle Diffusion Kinetic Model	86
3.5	Adsorption Isotherm	90
3.5.1	Langmuir Isotherm Model	94
3.5.2	Freundlich Isotherm Model	102
3.5.3	Dubinin-Radushkevich (D-R) Isotherm Model	105
3.6	Thermodynamics Study	110
3.7	Desorption Study	112
3.8	Adsorption Mechanism	
3.8.1	Adsorption of Tartrazine	115
3.8.2	Adsorption of MG	118
3.8.3	Adsorption of Copper (II) Ion	121
<b>CHAPTER FOUR: CONCLUSION</b>		<b>125</b>

<b>CHAPTER FIVE: RECOMMENDATION FOR FUTURE RESEARCH</b>	128
<b>REFERENCES</b>	129
<b>APPENDICES</b>	141

## LIST OF TABLES

		Page
Table 1.1	Maximum adsorption capacities for the adsorption of MG onto various types of adsorbent	7
Table 1.2	Maximum adsorption capacities for the adsorption of copper (II) ion onto various types of adsorbent	10
Table 2.1	The linearity range of tartrazine, MG and copper (II) ion	40
Table 3.1	Solubility of CCB beads in acid, basic and neutral medium	51
Table 3.2	Percentage of swelling of CCB beads in acid, basic and neutral medium	52
Table 3.3	The surface area and pore diameter of CCB beads	58
Table 3.4	Equilibrium time and maximum adsorption capacity for each adsorbate with three different concentrations	76
Table 3.5	Pseudo-first-order rate constant, calculated adsorption capacity, correlation coefficient and experimental adsorption capacity values for adsorption of tartrazine onto CCB beads	79
Table 3.6	Pseudo-first-order rate constant, calculated adsorption capacity, correlation coefficient and experimental adsorption capacity values for adsorption for adsorption of MG onto CCB beads	80
Table 3.7	Pseudo-first-order rate constant, calculated adsorption capacity, correlation coefficient and experimental adsorption capacity values for adsorption for adsorption of copper (II) ion onto CCB beads	81
Table 3.8	Pseudo-second-order constants, correlation coefficients and experimental adsorption capacity values for adsorption of tartrazine onto CCB beads	83
Table 3.9	Pseudo-second-order constants, correlation coefficients and experimental adsorption capacity values for adsorption of MG onto CCB beads	84
Table 3.10	Pseudo-second-order constants, correlation coefficients and experimental adsorption capacity values for adsorption of copper (II) ion onto CCB beads	85

Table 3.11	Intraparticle diffusion rate constants and correlation coefficients for adsorption of tartrazine, MG and copper (II) ion onto CCB beads	90
Table 3.12	Langmuir and Freundlich parameters for adsorption of tartrazine onto CCB beads	98
Table 3.13	Langmuir and Freundlich parameters for adsorption of MG onto CCB beads	98
Table 3.14	Langmuir and Freundlich parameters for adsorption of copper (II) ion onto CCB beads	99
Table 3.15	Separation factor, $R_L$ values for adsorption of tartrazine, MG and copper (II) ion onto CCB beads	101
Table 3.16	Dubinin-Radushkevich isotherm parameters for adsorption of tartrazine onto CCB beads	107
Table 3.17	Dubinin-Radushkevich isotherm parameters for adsorption of MG onto CCB beads	108
Table 3.18	Dubinin-Radushkevich isotherm parameters for adsorption of copper (II) ion onto CCB beads	109
Table 3.19	Values of Gibbs free energy, enthalpy and entropy change for adsorption of tartrazine, MG and copper (II) ion onto CCB beads	112
Table 3.20	Percentage of desorption for tartrazine, MG and copper (II) ion by using different desorbing agents	114

## LIST OF FIGURES

	Page
Figure 1.1	Molecular structure of tartazine 3
Figure 1.2	Molecular structure of MG 5
Figure 1.3	Chemical structure of chitin 11
Figure 1.4	Chemical structure of chitosan 12
Figure 1.5	Chemical structure of bentonite 15
Figure 2.1	Determination of P and P <sub>0</sub> from FTIR spectra of chitosan 33
Figure 3.1	pH <sub>ZPC</sub> plot for CCB beads 54
Figure 3.2	FTIR spectra for chitosan, bentonite and CCB beads 55
Figure 3.3	SEM images for bentonite at (a) 1000x and (b) 3000x magnification 57
Figure 3.4	SEM images for CCB beads at (a) 1000x and (b) 3000x magnification 57
Figure 3.5	N <sub>2</sub> adsorption-desorption isotherm plot of CCB beads 58
Figure 3.6	XRD patterns of (a) bentonite, (b) chitosan beads, (c) CCB beads 59
Figure 3.7	Proposed reaction path for preparation of CCB beads 61
Figure 3.8	Determination of precipitation pH for copper hydroxide 63
Figure 3.9	Effect of initial pH for the adsorption of tartrazine, MG and copper (II) ion onto CCB beads 65
Figure 3.10	Speciation of copper at various pH 66
Figure 3.11	Effect of stirring speed for the adsorption of tartrazine, MG and copper (II) ion onto CCB beads 68
Figure 3.12	Effect of adsorbent dosage for the adsorption of tartrazine onto CCB beads 70
Figure 3.13	Effect of adsorbent dosage for the adsorption of MG onto CCB beads 71

Figure 3.14	Effect of adsorbent dosage for the adsorption of copper (II) ion onto CCB beads	71
Figure 3.15	Effect of initial tartrazine concentration and contact time for adsorption of dyes onto CCB beads	74
Figure 3.16	Effect of initial MG concentration and contact time for adsorption of dyes onto CCB beads	75
Figure 3.17	Effect of initial copper (II) ion concentration and contact time for adsorption of dyes onto CCB beads	75
Figure 3.18	Pseudo-first-order plot for adsorption of tartrazine onto CCB beads	79
Figure 3.19	Pseudo-first-order plot for adsorption of MG onto CCB beads	80
Figure 3.20	Pseudo-first-order plot for adsorption of copper (II) ion onto CCB beads	81
Figure 3.21	Pseudo-second-order plot of adsorption of tartrazine onto CCB beads	83
Figure 3.22	Pseudo-second-order plot of adsorption of MG onto CCB beads	84
Figure 3.23	Pseudo-second-order plot of adsorption of copper (II) ion onto CCB beads	85
Figure 3.24	Intraparticle diffusion plot for adsorption of tartrazine onto CCB beads	88
Figure 3.25	Intraparticle diffusion plot for adsorption of MG onto CCB beads	89
Figure 3.26	Intraparticle diffusion plot for adsorption of copper (II) ion onto CCB beads	89
Figure 3.27	Adsorption isotherm for adsorption of tartrazine onto CCB beads	92
Figure 3.28	Adsorption isotherm for adsorption of MG onto CCB beads	93
Figure 3.29	Adsorption isotherm for adsorption of copper (II) ion onto CCB beads	93
Figure 3.30	Langmuir plots for adsorption of tartrazine onto CCB beads at 300, 310 and 320 K	96

Figure 3.31	Langmuir plots for adsorption of MG onto CCB beads at 300, 310 and 320 K	96
Figure 3.32	Langmuir plots for adsorption of copper (II) ion onto CCB beads at 300, 310 and 320 K	97
Figure 3.33	Freundlich plots for adsorption of tartrazine onto CCB beads at 300, 310 and 320 K	103
Figure 3.34	Freundlich plots for adsorption of MG onto CCB beads at 300, 310 and 320 K	104
Figure 3.35	Freundlich plots for adsorption of copper (II) ion onto CCB beads at 300, 310 and 320 K	104
Figure 3.36	Dubinin-Radushkavich isotherm plots for adsorption of tartrazine onto CCB beads at 300, 310 and 320 K	107
Figure 3.37	Dubinin-Radushkavich isotherm plots for adsorption of MG onto CCB beads at 300, 310 and 320 K	108
Figure 3.38	Dubinin-Radushkavich isotherm plots for adsorption of copper (II) ion onto CCB beads at 300, 310 and 320 K	109
Figure 3.39	Van't Hoff plots for adsorption of tartrazine, MG and copper (II) ion onto CCB beads	111
Figure 3.40	FTIR spectra for CCB beads before and after been loaded with tartrazine	115
Figure 3.41	Proposed mechanism for adsorption of tartrazine onto CCB beads at pH 2.5	117
Figure 3.42	SEM images for CCB beads (a) before been loaded with tartrazine at 3000x magnification (b) after been loaded with tartrazine at 1000x magnification	118
Figure 3.43	FTIR spectra for CCB beads before and after been loaded with MG	118
Figure 3.44	Proposed mechanism for adsorption of MG onto CCB beads at pH 6	120
Figure 3.45	SEM images for CCB beads (a) before been loaded with MG at 1000x magnification (b) after been loaded with MG at 3000x magnification	121
Figure 3.46	FTIR spectra for CCB beads before and after been loaded with copper (II) ion	122

Figure 3.47	Proposed mechanism for adsorption of copper (II) ion onto CCB beads at pH 4	122
Figure 3.48	SEM images for CCB beads (a) before been loaded with copper (II) ion at 3000x magnification (b) after been loaded with copper (II) ion at 1500x magnification	123
Figure 3.49	EDS spectrum obtained (a) before being loaded with copper (II) ion (b) after CCB beads were loaded with copper (II) ion	124

## LIST OF SYMBOLS AND ABBREVIATIONS

$\Delta G^\circ$	Gibbs free energy change ( $\text{kJ mol}^{-1}$ )
$\Delta H^\circ$	Enthalpy change ( $\text{kJ mol}^{-1}$ )
$\Delta \text{pH}$	Difference between initial pH and the final pH
$\Delta S^\circ$	Entropy change ( $\text{J K}^{-1} \text{mol}^{-1}$ )
A	Absorbance
$A_a$	Amount of adsorbates adsorbed (mg)
AAS	Atomic adsorption spectrophotometer
ADI	Acceptable daily intake
$A_r$	Amount of adsorbates released (mg)
b	Langmuir constant ( $\text{L mg}^{-1}$ )
BET	Brunauer-Emmett-Teller
BJH	Barrett-Joyner-Halenda
BOD	Biochemical oxygen demand
CCB	Chitosan coated bentonite
$C_e$	Equilibrium concentration ( $\text{mg L}^{-1}$ )
$C_o$	Initial concentration ( $\text{mg L}^{-1}$ )
COD	Chemical oxygen demand
d	Diameter
D-R	Dubinin-Radushkevich
E	Mean energy of adsorption ( $\text{kJ mol}^{-1}$ )
ECH	Epichlorohydrin
EDS	Energy dispersive spectrometer
EGDE	Ethylene glycol diglycidyl ether
ETAD	Ecological and Toxicological Association of the Dyestuff
FAO	Food and Agricultural Organization

FTIR	Fourier transform infrared spectrophotometer
GLA	Glutaraldehyde
h	Initial rate constant ( $\text{mg g}^{-1} \text{min}^{-1}$ )
$H_o$	Height of dry beads (cm)
$H_t$	Height of the swollen beads (cm)
IUPAC	International Union of Pure and Applied Chemistry
JECFA	Joint FAO/WHO Expert Committee on Food Additives
k	Adsorption energy ( $\text{mol}^2 \text{kJ}^{-2}$ )
$k_1$	Pseudo-first-order rate constant ( $\text{min}^{-1}$ )
$k_2$	Pseudo-second-order rate constant ( $\text{g mg}^{-1} \text{min}^{-1}$ )
$K_F$	Freundlich constant ( $\text{mg g}^{-1}$ )
$k_{id}$	Intraparticle diffusion constant ( $\text{mg g}^{-1} \text{min}^{-0.5}$ )
m	Weight (g)
MG	Malachite green
n	Adsorption intensity
$\text{pH}_o$	Initial pH of the solutions
$\text{pH}_{\text{slurry}}$	pH of aqueous slurry
$\text{pH}_{\text{ZPC}}$	pH of zero point charge
$q_e$	Equilibrium adsorption capacity ( $\text{mg g}^{-1}$ )
$q_{e, \text{calc}}$	Calculated equilibrium adsorption capacity ( $\text{mg g}^{-1}$ )
$q_{e, \text{exp}}$	Experimental equilibrium adsorption capacity ( $\text{mg g}^{-1}$ )
$q_m$	D-R adsorption capacity ( $\text{mg g}^{-1}$ )
$Q_{\text{max}}$	Maximum adsorption capacity ( $\text{mg g}^{-1}$ )
$q_t$	Adsorption capacity at time t ( $\text{mg g}^{-1}$ )
R	Gas constant ( $8.314 \text{ J K}^{-1} \text{mol}^{-1}$ )
$R^2$	Correlation coefficients
$R_L$	Separation factor

$R_p$	Percentage of removal (%)
S	Percentage of swelling
SEM	Scanning electron microscopy
T	Temperature (K)
t	Time (min)
V	Volume (L)
WHO	World Health Organization
XRD	X-ray diffraction
$\varepsilon$	Polanyi potential

# **PENYINGKIRAN TARTRAZINA, MALEKIT HIJAU DAN KUPRUM(II) MENGUNAKAN KOMPOSIT KITOSAN BENTONIT**

## **ABSTRAK**

Penjerapan tartrazina, malekit hijau (MG) dan ion kuprum (II) daripada larutan akueus dengan menggunakan manik komposit kitosan-bentonit terangkaisilang (CCB) telah dikaji. Manik CCB telah disediakan dengan melarutkan kitosan di dalam asid asetik 5 %. Bentonit kemudiannya ditambah ke dalam campuran dan campuran dibiarkan semalaman. Manik CCB kemudiannya dirangkaisilang dengan menggunakan larutan epiklorohidrin (ECH) sebelum dihancurkan, dikeringkan dan digunakan dalam kajian yang seterusnya. Pencirian manik CCB telah dilakukan dengan menggunakan analisis spektroskopi inframerah Fourier (FTIR) untuk mendapatkan maklumat berkaitan kumpulan berfungsi, analisis mikroskop elektron pengimbas (SEM) untuk mengetahui morfologi permukaan manik CCB, pengukuran luas permukaan Brunauer-Emmett-Teller (BET), analisis taburan saiz liang Barrett-Joyner-Halenda (BJH) dan analisis pembelauan sinar-X (XRD) bagi mendapatkan maklumat tentang kristaliniti manik CCB. Ujian keterlarutan dan pengembangan telah dilakukan untuk menentukan kestabilan manik CCB di dalam larutan berasid, berbes dan air suling. Selain daripada itu, nilai pH larutan akueus buburan ( $\text{pH}_{\text{buburan}}$ ) dan nilai pH titik sifar cas ( $\text{pH}_{\text{ZPC}}$ ) turut ditentukan dalam kajian ini. Jumlah zat terjerap yang dijerap dipengaruhi oleh pH larutan, kelajuan pengacauan, dos penjerap, masa penjerapan dan kepekatan awal zat terjerap. Faktor-faktor ini telah dikaji dalam kajian penjerapan berkelompok. Tiga jenis model kinetik telah

digunakan untuk data eksperimen iaitu model kinetik pseudo-tertib-pertama, pseudo-tertib-kedua dan pembauran antara zarah. Berdasarkan kajian kinetik, model pseudo-tertib-kedua sesuai dengan data eksperimen untuk kesemua zat terjerap. Di samping itu, tiga model isoterma telah digunakan dalam kajian ini; model isoterma Langmuir, Freundlich dan Dubinin-Radushkevich. Penjerapan tartrazina, MG dan ion kuprum (II) lebih sesuai dengan model Langmuir berbanding model Freundlich. Berdasarkan pengiraan, muatan penjerapan maksimum untuk tartrazina adalah 250.0, 277.8 dan 294.1 mg g<sup>-1</sup> masing-masing pada 300, 310 dan 320 K. Pada suhu yang sama, sebanyak 434.8, 555.6 dan 2500.0 mg g<sup>-1</sup> MG, dan 181.8, 434.8 dan 82.0 mg g<sup>-1</sup> ion kuprum (II) terjerap pada manik CCB. Penjerapan kedua-dua jenis pewarna adalah disebabkan oleh penjerapan kimia, manakala penjerapan ion kuprum (II) adalah disebabkan oleh pertukaran ion. Berdasarkan kajian kesan suhu terhadap proses penjerapan, penjerapan tartrazina, MG dan ion kuprum (II) adalah bersifat eksoterma dan proses berlaku secara spontan. Ujian penyaherapan telah dilakukan dengan menggunakan larutan EDTA, H<sub>2</sub>SO<sub>4</sub> dan NaOH yang berlainan kepekatan. Hanya ion kuprum (II) boleh dinyaherapkan daripada manik CCB oleh agen-agen penyaherap. Tartrazina dan MG tidak boleh dinyaherap daripada manik CCB.

# **CHITOSAN-BENTONITE COMPOSITE FOR THE REMOVAL OF TARTRAZINE, MALACHITE GREEN AND COPPER(II) FROM AQUEOUS SOLUTION**

## **ABSTRACT**

Adsorption of tartrazine, malachite green (MG) and copper (II) ion from aqueous solutions by chitosan-bentonite composite (CCB) beads was investigated. CCB beads were prepared by dissolving chitosan with 5 % acetic acid. Bentonite was then added into the mixture and left overnight. The beads were then cross-linked with epichlorohydrin (ECH) solution before ground, dried and used for the adsorption studies. CCB beads were characterized by Fourier transform infrared (FTIR) spectroscopy in order to determine the functional groups, scanning electron microscopy (SEM) for the information of surface morphology, Brunauer-Emmett-Teller (BET) surface area measurement, Barrett-Joyner-Halenda (BJH) pore size distribution analysis and X-ray diffractometry (XRD) in order to obtain the information regarding the crystallinity. Solubility and swelling tests were carried out to determine the stability of CCB beads in acid solution, basic solution and distilled water. Besides, the value of pH of aqueous slurry ( $\text{pH}_{\text{slurry}}$ ) and pH of zero point charges ( $\text{pH}_{\text{ZPC}}$ ) were also determined in this study. The amount of adsorbates adsorbed were influenced by initial pH of the solution, stirring speed, adsorbent dosage, contact time and initial adsorbate concentration. These were studied in batch adsorption study. Three types of kinetic model were implemented to the experimental data which were pseudo-first-order, pseudo-second-order and

intraparticle diffusion kinetic models. Based on the kinetic study, pseudo-second-order models agreed well with the experimental data for all adsorbates. On the other hand, three isotherm models were used in isotherm study; Langmuir, Freundlich and Dubinin-Radushkevich isotherm model. Tartrazine, MG and copper (II) ion fitted well with Langmuir model compared to Freundlich model. Based on the calculation, the maximum adsorption capacity for tartrazine were 250.0, 277.8 and 294.1 mg g<sup>-1</sup> at 300, 310 and 320 K respectively. At the same temperatures, 434.8, 555.6 and 2500.0 mg g<sup>-1</sup> of MG and 181.8, 434.8 and 82.0 mg g<sup>-1</sup> of copper (II) ion were adsorbed onto CCB beads. Adsorption of both types of dyes were due to chemisorption while the adsorption of copper (II) ion was by ion-exchange. From the temperature study, the adsorption of tartrazine, MG and copper (II) ion onto CCB beads were found to be exothermic in nature and occur spontaneously. Desorption tests were carried out at different concentrations of EDTA, H<sub>2</sub>SO<sub>4</sub> and NaOH solutions. Only copper (II) ion could be desorbed from CCB beads by using these desorbing agents but not for tartrazine and MG.

## **CHAPTER ONE**

### **INTRODUCTION**

#### **1.1 Water Pollution**

It is well mentioned that 75 % of the earth is covered by water but nowadays most of the water supplies are contaminated. In many industrialized areas for instance, large amount of untreated wastewater are discharged into the water stream. Moreover, some chemicals released from the factories are absorbed into the soil which consequently polluted the underground water sources. The polluted water supply will cause a trouble for human beings in search of clean drinking water because throughout history, the quality of drinking water has become a factor in determining human welfare (Manahan, 1984). Hence, the unhygienic water sources are not only a nuisance for a human beings but it is also a threat for the aquatic lives.

Water pollution is caused by the presence of the pollutant. Pollutant is a substance that is present in higher than natural concentration resulting from human activities. It also has a net detrimental effect upon its environment or upon something of value in that environment (Manahan, 1984). Pollutants can be metal ions, coloured matters, odoured matters, pesticides, detergent, and petroleum wastes. This study is focused on the pollution which caused by dyes and metal ion.

## 1.2 Dyes

Approximately 10,000 different dyes and pigments are used by industries and over  $7 \times 10^5$  tons of dyes are annually produced worldwide (Mane et al., 2007). They are extensively used in many industries such as the textile, leather, paper production, food technology, etc (Hameed & Lee, 2009). The textile industry alone accounts for two thirds of the total dyestuff production and about 10–15 % of the dyes were used through the effluent (Lata et al., 2007). More surprisingly, over 90 % of some 4000 dyes tested in an ETAD (Ecological and Toxicological Association of the dyestuff) survey had  $LD_{50}$  values greater than  $200 \text{ mg kg}^{-1}$  (Shore, 1996).

With the increase of the dyes usage, the discharge of dyes into water bodies becomes uncontrollable. It can impede light penetration into waters, retard photosynthesis activity, inhibit the growth of biota and has a tendency to chelate metal ions (Garg et al., 2004; McKay et al., 1980). In fact, the highly coloured effluent released to the water bodies also coupled with high chemical and biochemical oxygen demand (COD and BOD) and suspended solid (Hamdaoui et al., 2008; Wong & Yu, 1999).

Most of dyes are synthesized from organic substances and have complex structure. Generally, dyes can be classified with regard to their chemical structure such as azo, anthraquinone, indigo, and triphenyl methane. They are also classified according to the method and domain of usage; acid, basic, direct, reactive, chromic, metal-complexes, disperse, mordant, sulfur, vat and pigment. Due to their complex structure and synthetic

origins, dyes are designed to resist breakdown with time and exposure to sunlight, water, soap, aerobic digestion and oxidizing agent, they cannot be easily removed by conventional wastewater treatment process (Crini & Badot, 2008; Wang & Wang, 2007a).

### 1.2.1 Tartrazine

Tartrazine or the International Union of Pure and Applied Chemistry (IUPAC) name trisodium-5-hydroxy-1-(4-sulfonatophenyl)-4-(4-sulfonatophenylazo)-H-pyrazole-3-carboxylate is categorized as an acid dye. It is also known as Acid Yellow 23 with the empirical formula  $C_{16}H_9N_4O_9S_2Na_3$  and molecular weight  $534.4 \text{ g mol}^{-1}$ . The molecular structure of tartrazine is given in Fig. 1.1.

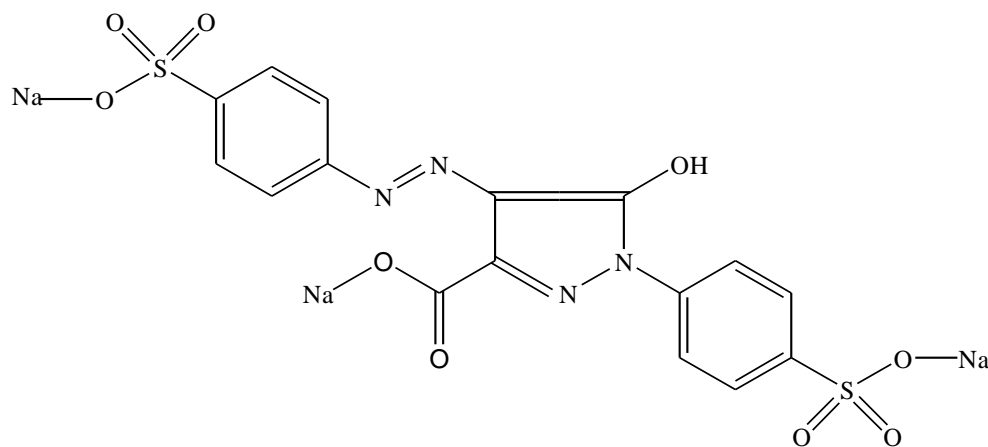


Fig. 1.1: Molecular structure of tartazine (Wawrzkieicz & Hubick, 2009)

Due to the lower price compared to beta carotene, tartrazine is widely used as food additives. Tartrazine is commonly found in food stuffs such as soft drinks, instant

pudding, flavored chips, custard powder, soup sauces, ice cream, candy, chewing gum, marzipan jam, jelly, marmalade, mustard and confectionary products. Besides, products like drugs, hair products, moisturizers, toys for kids and crayon also uses tartrazine thoroughly. Textile, electroplating and pharmaceuticals industries also not exceptional from using this health threatening dye (Wawrzekiewicz & Hubick, 2009; Mittal et al., 2006; Monser & Adhoum, 2008; Elhkim et al., 2007).

The presence of an azo ( $-N=N-$ ) group in tartrazine structure possesses high toxicity which is why it becomes a threat to human beings and fauna. Apart from acting as a catalyst in hyperactivity and other behavioural problems, tartrazine also can cause asthma, migraines, eczema, thyroid cancer, and lupus (Mittal et al., 2006). Since tartrazine is very harmful for living thing, Joint FAO/WHO Expert Committee on Food Additives (JECFA) had stated that an acceptable daily intake (ADI) for tartrazine is 0-7.5 mg kg<sup>-1</sup> body weight (Elhkim et al., 2007).

Even tartrazine possesses hazardous effect towards human being, very less study for the removal of tartrazine from wastewater have been done by researchers. Mittal et al. (2006) studied the removal of tartrazine from aqueous solution by using bottom ash and de-oiled soya. They found that 86.85 and 85.31 % of tartrazine were adsorbed from bottom ash and de-oiled soya, respectively. Besides, by using hen feather as another alternative, almost 100 % of tartrazine was adsorbed at lower concentration ( $3 \times 10^{-5}$  M), and 47 % of tartrazine were adsorbed at higher concentration ( $1.0 \times 10^{-4}$  M) (Mittal et al., 2007). Wawrzekiewicz & Hubicki (2008) is the other researchers who studied the

adsorption of tartrazine from the wastewater. They used polystyrene anion exchangers as the adsorbent for the adsorption of tartrazine. They reported that 50 mg g<sup>-1</sup> of tartrazine adsorbed from the aqueous solution.

More research for the adsorption of tartrazine from the wastewater need to be done by researchers. Because of that, we will use chitosan coated bentonite (CCB) beads for the adsorption of tartrazine from the aqueous solutions.

### 1.2.2 Malachite Green

Malachite green (MG) or Basic Green 4 is a basic dye. It is also known as N, N, N', N'-tetramethyl-4, 4'-diaminotriphenyl carbonium. The empirical formula for MG is C<sub>25</sub>H<sub>26</sub>N<sub>4</sub>O<sub>2</sub> and molecular weight 326.42 g mol<sup>-1</sup>. Fig. 1.2 shows the molecular structure of MG.

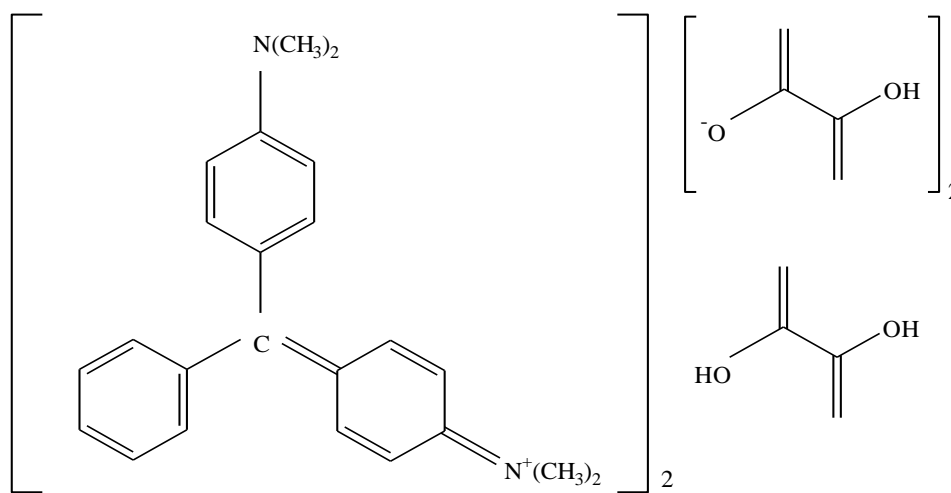


Fig. 1.2 Molecular structure of MG (Hamdaoui et al., 2008)

MG is widely used to dye wool, silk, cotton and leather in textile industries and also as a strong anti-fungal, anti-bacterial and anti-parasitical agent in fish farming (Mall et al., 2005; Mittal, 2006). Besides, MG is also applied on the wounds and ulcer as an antiseptic (Hamdaoui et al., 2008).

Nowadays, MG is considered as a highly controversial compound due to its genotoxic and carcinogenic properties (Bekçi et al., 2008a). It can cause mutagenesis, teratogenesis, respiratory toxicity, muscle glycogenolysis, impairs protein synthesis and tumor promoter. Severe damage to liver, gill, kidney, intestine, gonads, and pituitary gonadotrophic cell might also occur to human beings. Besides, the aquatic lives are threatened by MG which cause to the degenerative changes in fishes (Kannan et al., 2008; Hamdaoui et al., 2008; Srivasta et al., 2008).

Due to the hazardous effects arise from MG usage, the removal of MG from water bodies become environmentally important. Some researchers have come out with various adsorbents. Table 1.1 shows maximum adsorption capacities recorded by previous researchers by using various types of adsorbent. Based on Table 1.1, the highest adsorption capacity was recorded by Bulut et al. (2008). By using oil palm trunk fibre for the adsorption of MG  $178.6 \text{ mg g}^{-1}$  maximum adsorption capacity was recorded. In searching of better adsorbent, we will use CCB beads for MG adsorption in order to make this adsorbent comparable with other adsorbents.

Table 1.1: Maximum adsorption capacities for the adsorption of MG onto various types of adsorbent

Adsorbents	$Q_{\max}$ (mg g <sup>-1</sup> )	References
Bentonite	178.6	Bulut et al., 2008
Oil palm trunk fibre	149.4	Hameed & El-Khaiary, 2008c
Cyclodextrin-based material	91.9	Crini et al., 2007
Native anaerobic granular sludge	61.7	Cheng et al., 2008
Heat-treated anaerobic granular sludge	59.2	Cheng et al., 2008
Aerobic granules	56.8	Sun et al., 2008
Sawdust ( <i>Hevea brasiliensis</i> )	36.5	Kumar & Sivanesan, 2007
Dead pine needles	33.6	Hamdaoui et al., 2008
<i>Caulerpa racemosa</i> var. <i>cylindracea</i>	25.7	Bekçi et al., 2008b
Arundo donax root carbon	8.69	Zhang et al., 2008

### 1.3 Heavy Metal Ion

Water pollution due to toxic heavy metals remains a serious environmental and public problem nowadays. Heavy metals such as lead, copper, zinc, cadmium and nickel are among the most toxic pollutants present in marine, ground and industrial wastewater (Kumar et al., 2006). They come from various industrial sources such as electroplating, metal finishing, textile, storage batteries, lead smelting, mining, plating, ceramic, and glass industries (Kensinkankan et al., 2003).

The toxicity of heavy metal will effect even at low concentration. Heavy metal can accumulate throughout the food chain, which can lead to serious ecological and health problem. The presence of heavy metal ions in an aqueous system, can be readily absorbed into human body making this problem even worse. Even a very small amount of heavy metal ions can cause severe physiological or neurological damage (Larous et al., 2005; Wong et al., 2003)

### **1.3.1 Copper**

Copper is widely used industrial metal. The properties of copper which make it suitable for many applications including high electrical and thermal conductivity, good corrosion resistant, easy for fabrication and installation, attractive appearance, ready availability and high recyclability. Due to its good properties, copper is widely used in many industries such as electroplating, metal cleaning plating bath, mining, fertilizers, pulp and paper, petroleum, air conditioning, tubing, and roofing industries. It is reported that the concentration of copper ion in these wastewater can reach up to 1000 mg L<sup>-1</sup> (Kumar et al., 2006; Özer et al., 2004).

Although copper is essential for human life, the excess exposure to the copper ion still harmful for human life. It is considered to be non-toxic for man unless it exceeds 5 mg L<sup>-1</sup> (Ajmal et al., 2005). The excessive copper discharge might be found as a contamination in food especially shellfish, liver, mushrooms, nuts and chocolate. In

conjunction, any process or container which uses copper material may contaminate the product itself (Nuhoglu & Oguz, 2003; Ozsoy & Kumbur, 2006).

Some researchers have comprehensively reviewed the toxicity of copper in human. Acute copper poisoning can cause stomach and intestinal distress, kidney damage, anemia, fever with influenza syndrome, irritation of upper respiratory tract, gastrointestinal disturbance with vomiting and diarrhea and a form of contact dermatitis (Kumar et al., 2004; Ozsoy & Kumbur, 2006; Rengaraj et al., 2004). On the other hand, prolonged copper ion inhalation increase the tendency of having lung cancer (Nuhoglu & Oguz, 2003). Because of the toxicity of copper, World Health Organization (WHO) has stated that drinking water should contain less than  $1 \text{ mg L}^{-1}$  copper (II) ion.

Table 1.2 shows some studies to adsorb copper (II) ion from aqueous solution with various types of adsorbent that have been done by other researchers. Even many researchers studied the adsorption of copper (II) ion by using various types of adsorbents, but very few of them recorded adsorption capacity higher than  $100 \text{ mg g}^{-1}$ . In this study, beside of trying to remove the maximum copper ion according to World Health Organization (WHO) guideline, we also want to use CCB beads as one of the adsorbent which is comparable with other low cost adsorbents.

Table 1.2: Maximum adsorption capacities for the adsorption of copper (II) ion onto various types of adsorbent

Adsorbents	$Q_{\max}$ (mg g <sup>-1</sup> )	References
Orange peel-methyl acrylate	289.0	Feng et al, 2009
Chitosan coated perlite	196.1	Kalyani et al., 2005
<i>Spirogyra</i>	133.3	Gupta et al., 2006
Chitosan coated perlite	104	Hasan et al., 2008
Modified bagasse	101.0	Jiang et al., 2009
Teak leaves powder	95.4	King et al., 2006
Chitosan-alginate	67.7	Wan Ngah & Fatinathan, 2008
Chitosan	64.6	Wan Ngah & Fatinathan, 2008
Bentonite-2,2'-dipyridyl	54.1	Erdem et al., 2008
Dehydrated wheat bran	51.5	Özer et al., 2004
Tea waste	48.0	Amarasinghe & Williams, 2007
Bentonite	44.8	Veli & Alyüz, 2007
Cross-linked metal-complex chitosan	33.0	Chen et al., 2009
Chitosan-GLA	31.2	Wan Ngah & Fatinathan, 2008
Sunflower stalks	29.3	Sun & Shi, 1998
Tartaric acid modified rice husl	29.0	Wong et al., 2003
<i>Ulva fasciata</i> sp.	26.9	Kumar et al., 2006
Base treated rubber leaves	14.9	Wan Ngah & Hanafiah, 2008
Cotton ball	11.4	Ozsoy & Kumbur, 2006
Tree fern	10.6	Ho et al., 2002
Maple wood sawdust	9.5	Rahman & Islam, 2009

## 1.4 Chitin and Chitosan

Chitin is the second most abundance natural polymer after cellulose. It can be found in the exoskeleton of marine life, the cuticles of insect, and the cell wall of fungi. This low cost material is a linear homopolymer composed of  $\beta(1-4)$ -linked N-acetyl glucosamine (Fig. 1.3). It is structurally similar to cellulose, but it is an aminopolymer and has acetamido groups at C-2 positions instead of hydroxyl groups in cellulose structure (Crini & Badot, 2008).

Chitin is low in toxicity, biodegradable, antibacterial, hydrophilic and has good affinity for protein. Due to these good properties, chitin is commonly used in many industries such as enzyme immobilizations in food industries, for clarification of fruit juices and milk processing, isolation of lectine, wound healing, biosensors and to adsorb silver thiosulfate complexes and actinides in industrial pollutants (Rinaudo, 2006; Sangkroah et al., 2004; Krajewska, 2004).

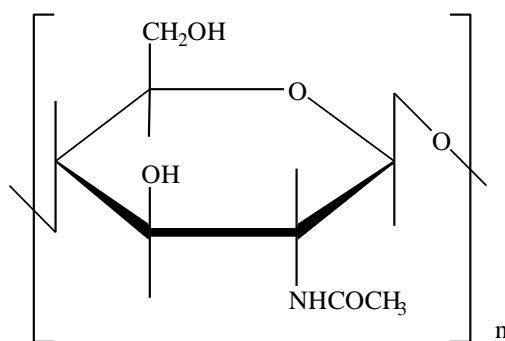


Fig. 1.3: Chemical structure of chitin (Crini & Badot, 2008)

Unfortunately, chitin is extremely insoluble material. Its insolubility is a major problem that confronts of processes and uses of chitin (Rinaudo, 2006). Thus, chitin has been derived to chitosan. Chitosan is obtained by deacetylating the acetamido group in chitin by using strong alkaline solution such as sodium hydroxide solution. Chitin only labeled as chitosan when the deacetylation degree greater than 65 %, where only beyond this deacetylation degree chitosan will be soluble in acid solutions (Wan Ngah & Fatinathan, 2008; Wan Ngah et al., 2004; Guibal, 2004).

Chitosan or poly ( $\beta$ -1-4)-2-amino-2-deoxy-D-glucopyranose (Fig. 1.4) was found as non-toxic, biological tolerance, renewable, hydrophilic, biocompatible, biodegradable and anti-bacterial (Rinuado, 2006; Uzun & Güzel, 2005). These features are almost similar with the features of chitin. Additionally, the performance of chitosan is expected to be better compared to chitin because the amine ( $-NH_2$ ) groups in chitosan are much more reactive than the acetamide ( $-NHCOCH_3$ ) groups on chitin. The free electron doublet of nitrogen on amine groups is responsible for the adsorption cations, whereas the protonation of amine groups in acidic medium is responsible for the adsorption of anions (Guibal, 2004).

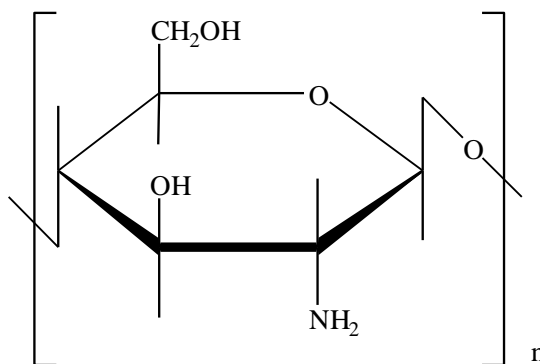


Fig. 1.4: Chemical structure of chitosan (Crini & Badot, 2008)

Since chitosan exhibited many good features, it becomes very useful to many industries such as agricultural, water and waste treatment, food and beverages, cosmetics and toiletries and biopharmaceuticals. In agricultural field, chitosan is used to stimulate the plant growth, coat the seeds and protect the plant from frost. Interestingly, chitosan also very useful in skin protection such as maintaining the moisture of the skin, treat the acne, giving good tone of the skin, etc and hair care in cosmetics industries. Besides, applications of chitosan in biopharmaceutical, food, and beverages industries are undoubtedly (Rinaudo, et al., 2006).

Chitosan act as antitumoral, bacteriastatic, lipid binder, preservatives thicker, stabilizer, etc in these industries. Meanwhile, some potential biomedical applications such as surgical sutures, dental implants, artificial skin, bone rebuilding, corneal contact lenses and drug releaser for humans and animals by using chitosan is still under observations (Rinaudo, 2006).

Wastewater treatment is another industry which applied chitosan widely. Chitosan has been reported for high potential of adsorption of dyes, metal ions and protein. Good adsorption performance is due to the presence of the amine ( $-NH_2$ ) and hydroxyl ( $-OH$ ) groups which can serve as the coordination or adsorption sites (Chang & Juang, 2004).

## 1.5 Bentonite

Clay minerals are made up of hydrous aluminosilicates sheets. It has been used in many industrial areas such as an emulsifier agent for asphaltic and resinous substances, as an adhesive agent in horticultural sprays and insecticides, in concrete mixtures, as a plasticizer in ceramic bodies and as a bleaching in vegetables oils and drilling mud. Besides, clays also have been accepted as one of the appropriate low cost adsorbents for removal of contaminant from wastewater. The wide usefulness of clay mineral is essentially a result of high specific surface area, high chemical and mechanical stabilities and a variety of surface and structural properties (Futalan et al., 2011a; Montes-H & Geraud, 2004; Bulut et al., 2008).

Bentonite (Fig. 1.5) is known as a clay mineral consisting of smectite mineral of montmorillonite group (Montes-H & Geraud, 2004). The inner layer of bentonite is composed of an octahedral sheet situated between two  $\text{SiO}_4$  tetrahedral sheets. Substitutions within the lattice structure of  $\text{Al}^{3+}$  for  $\text{Si}^{4+}$  in the tetrahedral sheet and  $\text{Mg}^{+}$  for  $\text{Al}^{3+}$  in the octahedral sheet result in unbalanced charges in the units of bentonite surface. The charge imbalance is compensated by exchangeable cations including  $\text{H}^{+}$ ,  $\text{Na}^{+}$  or  $\text{Ca}^{2+}$  on the surface (Erdem et al., 2008).

Among the clays studied, bentonite has received considerable recognition as an adsorbent (Bulut et al., 2008). Since it is a good adsorbent, some researchers have come out with modifications of bentonite. One of the modifications which captured our

interest is the coating of bentonite with chitosan (Gecol et al., 2008; Futralan et al., 2011a; Futralan et al., 2011b)

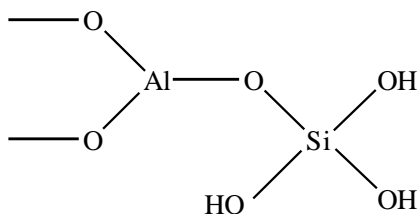


Fig. 1.5: Chemical structure of bentonite (Erdem et al., 2008)

## 1.6 Modifications of Chitosan

Wastewater treatment is one of the industries which applied chitosan widely. Researchers have been trying to adsorb many pollutants including dyes and heavy metal ions by using this low cost adsorbent. As time passed, many modifications have been built up in order to enhance the chitosan performance as low cost adsorbent. Modifications of chitosan could include physical and chemical modifications.

Chemical modifications briefly done in order to prevent chitosan from dissolve in acid medium, improve the adsorption capacities and enhance the adsorption selectivity. Besides, the resistance of cross-linked chitosan towards biochemical and microbiological degradation also increased (Guibal, 2004; Guibal et al., 2000; Yang & Yuan, 2001).

The cross-linking procedure may be performed by reaction of chitosan with different types of cross-linking agents such as glutaraldehyde (GLA) (Guibal et al., (1999); Wan Ngah et al., 2002b; Wan Ngah & Fatinathan, 2008; Wu et al., 2001), ethylene glycol diglycidyl ether (EGDE) (Tianwei et al., 2001; Wan Ngah et al., 2002b), alginate (Wan Ngah & Fatinathan, 2008) and tripolyphosphate (Wan Ngah & Fatinathan, 2010). In the other hand, mono-functional reagents such as epichlorohydrin (ECH) also been used by Wan Ngah et al. (2002b) and Chiou & Li (2002).

Unfortunately, not all cross-linking step by using cross-linking agents exhibited the increasing of the adsorption capacities, especially for the cross-linking agents which react with amine groups such as GLA (Guibal, 2004). For this reason, the researchers have been encouraged to come out with other modification which can improve the performance of chitosan as the adsorbent.

One of the alternative ways to improve the performance of chitosan other than using cross-linking agent is by impregnating chitosan with other materials. Many types of materials were used to modify chitosan such as alumina (Shi et al., 2003; Boddu et al., 2003; Boddu et al., 2008), montmorillonite (Fan et al., 2006, Wang & Wang, 2007a; Wang & Wang, 2007b), perlite (Hasan et al., 2003; Kalyani et al., 2005),  $\text{Fe}_3\text{O}_4$  (Chang & Chen, 2005; Chang & Chen 2006; Zhi et al., 2006), activated carbon (Nomanbhay & Palasamy, 2005; Vinitnantharat et al., 2007), bentonite (Gecol et al., 2006), sand (Wan et al., 2004), cellulose (Li & Bai, 2005), loofah fiber (Chang & Juang, 2005), anionic/nonionic surfactant (Chatterjee et al., 2009) and activated clay (Chang & Juang, 2004).

These modifications are believed can increase the sorption properties. It is because gel formation decreases the crystallinity of the adsorbent and thus enhances the expansion of the porous network in the adsorbent (Guibal et al., 2000; Yang & Yuan, 2001). Besides, Nomanbhay and Palasamy (2005) who worked on modification of chitosan with activated carbon claimed that the surface modifications have added the economical value, can reduce the cost of waste disposal and most importantly provide potential inexpensive alternatives to existing commercial activated carbon. The combination of these materials also known as composite chitosan which will be discussed more in section 1.7.

Instead of modifying chitosan chemically, it also can be modified by physical modification. Physical modifications of chitosan can be done by preparing different polymer conditions such as gel beads, membranes, sponge, honeycomb fibers etc. The control of polymer conditioning may help in designing the sorption process (Guibal, 2004).

In this study, we would like to focus on preparing chemically modified chitosan by embedding other materials onto chitosan surface or also known as chitosan composite.

## **1.7 Chitosan Composites**

### **1.7.1 Chitosan-Alumina/Silica Composite**

One of a good characteristics of alumina/silica is they are porous in nature. The large and narrow pore size distribution in the particles can increase the macromolecular transfer inside the matrix (Shi et al., 2003). Because of this good properties, Shi et al. (2003) and Boddu et al. (2003; 2008) had innovatively embedded alumin/silicaa in order to produce composite chitosan-alumina biosorbent.

Both Shi et al. (2003) and Boddu et al. (2003; 2008), used different methods of preparing this composite chitosan-alumina/silica. Shi et al. (2003) used three important steps while preparing composite chitosan-alumina which were (i) the preparation of chitosan-alumina/silica composite, (ii) the cross-linking with glutaraldehyde and (iii) copper (II) ion immobilization. On the other hand, Boddu et al. (2003; 2008) used oxalic acid to replace acetic acid to dissolve the chitosan. According to them, oxalic acid will act as a bridge between alumina/silica and chitosan.

The composites were characterized in order to know some properties. Boddu et al. (2003; 2008) found that the surface area, pore volume, and pore diameter of the beads were  $125.24 \text{ m}^2 \text{ g}^{-1}$ ,  $0.1775 \text{ cm}^3 \text{ g}^{-1}$ , and  $71.125 \text{ \AA}$ , respectively. While, based on the values of the specific surface area, Shi et al. (2003) concluded that the surface area of silica dropped after being coated with chitosan from  $62.0$  to  $58.9 \text{ m}^2 \text{ g}^{-1}$ .

According to batch adsorption studies by Boddu et al. (2003; 2008), the maximum adsorption capacity of chromium (VI), arsenic (III) and arsenic (V) ions increased by using composite chitosan-alumina compared to adsorption by unmodified chitosan which were 153.8, 56.5, and 96.5 mg g<sup>-1</sup> to 78.0, 0.0 and 58.0 mg g<sup>-1</sup> respectively. From these observations, the preparation of composite chitosan-alumina could improve the performance of chitosan in the adsorption study.

### **1.7.2 Chitosan-Montmorillonite Composite**

Other than alumina/silica, montmorillonite is another type of natural phyllosilicates. Fan et al. (2007) and Wang and Wang (2007a; 2007b) have developed chitosan coated montmorillonite for the adsorption studies.

Wang and Wang (2007a; 2007b) discussed the effect of chitosan to montmorillonite ratio in the composition of the adsorbent. The density and surface area decreased with an increasing in the molar ratio of chitosan and montmorillonite. Besides, they discovered that flocculated-interchelated nanostructure formed at high montmorillonite content and interchelate-exfoliated nanostructure formed at low montmorillonite content. This is the same observation obtained by Wang et al. (2005).

Wang and Wang (2007a; 2007b) finally chose 5:1 and 1:10 of chitosan to montmorillonite molar ratio for the subsequent studies. Maximum adsorption capacities for both ratios were 54.52 and 290.8 mg g<sup>-1</sup>. Fan et al. (2007) who studied the adsorption

of chromium (VI) ion onto composite chitosan-montmorillonite found that chromium (VI) ion was physically attached to the composite. Maximum adsorption capacity for adsorption of chromium (VI) ion onto composite chitosan-montmorillonite was 34.86 mg g<sup>-1</sup> and the adsorption process was favourable at lower temperature.

### **1.7.3 Chitosan-Perlite Composite**

Development of composite chitosan-perlite was done by mixing chitosan and perlite with 1 to 2 weight ratio (Hassan et al., 2003; Kalyani et al., 2005). Once the composite chitosan-perlite obtained, several characterization have been done onto it. Based on the high-temperature pyrolysis, 23 % of chitosan was found coated on perlite in composite chitosan-perlite beads (Hassan et al., 2003). The surface morphology of pure perlite was found changed significantly after being coated with chitosan. Before the coating, pure perlite powder does not have any particular shape of crystalline structure, but after the coating process between chitosan and perlite, the surface became porous (Hassan et al., 2003).

By coating chitosan on perlite, more active sites could be effectively exposed for adsorption process. This was proved based on the maximum adsorption capacities recorded which were 153.8 mg g<sup>-1</sup> of chromium (VI) ion adsorbed by chitosan coated perlite instead of only 78.0 mg g<sup>-1</sup> chromium (VI) ion adsorbed by unmodified chitosan (Hassan et al., 2003). High adsorption capacities were also obtained by Kalyani et al.

(2005) whereby 196.07 and 114.94 mg g<sup>-1</sup> were recorded for adsorption of copper (II) and nickel (II) ions respectively.

#### **1.7.4 Chitosan-Fe<sub>3</sub>O<sub>4</sub> Composite**

Monodisperse chitosan coated Fe<sub>3</sub>O<sub>4</sub> was prepared by Chang and Chen (2005; 2006) and Zhi et al. (2006). According to Chang and Chen (2006), chitosan has no suitable functional groups to bind directly onto Fe<sub>3</sub>O<sub>4</sub> nanoparticles, thus they need to prepare carboxymethyl chitosan first. The carboxymethyl chitosan were then used bonded covalently with Fe<sub>3</sub>O<sub>4</sub> via carbodiimide activation. In fact, Fe<sub>3</sub>O<sub>4</sub> itself were prepared by co-precipitating Fe<sup>2+</sup> and Fe<sup>3+</sup> ions by ammonia solution before being treated under hydrothermal conditions.

Based on the characterizations, the mean diameter of the particles is 13.5 nm with 4.95 % chitosan coated on Fe<sub>3</sub>O<sub>4</sub> (Chang & Chen, 2006). In the other hand, Zhang et al., (2006) found that the diameter of composite decreased where before being coated with chitosan, the diameter of chitosan varied from 60 to 80 nm, but after preparation of composite chitosan-Fe<sub>3</sub>O<sub>4</sub>, the diameter of composites decreased to 10 to 50 nm.

Chang and Chen (2006) reported that 59.52 mg g<sup>-1</sup> gold (III) ion was adsorbed from the solution by using chitosan coated Fe<sub>3</sub>O<sub>4</sub>. Besides, faster equilibrium time was attained by using this adsorbent, whereby only 30 min was required to reach the equilibrium stage.

### **1.7.5 Chitosan-Activated Carbon Composite**

Nomanbhay and Palasamy (2005) have prepared chitosan coated oil palm shell charcoal while Vinitnantharat et al. (2007) prepared chitosan coated carbon from two types of granular activated carbon (GAC) which were from coconut shells and bituminous coal.

Nomanbhay and Palasamy (2005) reported that about 21 % chitosan was loaded on the oil palm shell charcoal by weight. The shape of the adsorbent was nearly spherical and diameter of the particle was found ranging 100-150  $\mu\text{m}$ . Besides, they also claimed that the removal of heavy metal ions could be improved by using palm oil shell for the modification of the chitosan surface.

In the other hand, Vinitnantharat et al. (2007) who prepared chitosan coated GAC found that chitosan was partially attached onto GAC surface and shielded some of the opening pores. The GAC surface modification resulted in increasing adsorption capacity compared to uncoated GAC. This is due to introduction of amine ( $-\text{NH}_2$ ) groups onto the carbon surface.

## **1.8 Adsorption**

There are many conventional methods used for the waste water treatment such as oxidation, reduction, precipitation, membrane filtration, ion exchange and adsorption. But, for the past two decades, adsorption techniques have been found to be superior for

the removal of contaminants compared to other techniques in terms of cost, design, ease of operation and insensitivity to toxic substances (Boujelben et al., 2009; Mittal et al. 2005; Wawrzkievicz and Hubicki, 2009).

Adsorption is the ability of certain solids to selectively concentrate solute from solution onto their surface (Gerente et al, 2007). In the earlier stage of the adsorption study, researchers need to develop an adsorbent and ensure that the adsorbent is stable in any media. After the adsorbent obtained, several characterizations are done onto adsorbents. Then, the adsorption studies proceed to the other stages.

At the first stage of the adsorption study, the optimum conditions, such as pH, stirring rate, adsorbent dosage and contact time were determined. Data from effect of contact time are then used for the kinetics study. Based on the kinetic study, the adsorption rate and rate-limiting step could be determined.

The maximum adsorption capacity of the adsorbate is the most important parameter in the adsorption study. It can be obtained from the isotherm study. Isotherm study also gives the information about adsorption mechanism, the surface properties and affinity towards adsorbate (Ho et al., 2002).

### 1.8.1 Adsorption Kinetics

In order to investigate the mechanisms of adsorption and potential rate-limiting steps such as mass transport and chemical reaction process, kinetics model have been used to test the experimental data. Three types of kinetics models were applied in this study, which were:

- (i) pseudo-first-order kinetic model (Ho & McKay, 1998a):

$$\log (q_e - q_t) = \log q_e - \frac{k_1}{2.303} t \quad (1.1)$$

- (ii) pseudo-second-order kinetic model (Ho & McKay, 2000)

$$\frac{t}{q_t} = \frac{1}{h} + \frac{1}{q_e} t \quad (1.2)$$

- (iii) intraparticle diffusion kinetic model (Weber & Morris, 1963)

$$q_t = k_{id} t^{0.5} \quad (1.3)$$

Based on the equations,  $q_e$  is the amount of the adsorbate adsorbed ( $\text{mg g}^{-1}$ ) at equilibrium,  $q_t$  is the amount of adsorbate adsorbed ( $\text{mg g}^{-1}$ ) at time  $t$  (min),  $k_1$  is the pseudo-first-order rate constant ( $\text{min}^{-1}$ ) and  $k_{id}$  is intraparticle diffusion constant ( $\text{mg g}^{-1}$

$\text{min}^{-0.5}$ ). In equation 1.2,  $h = k_2 q_e^2$  can be regarded as the initial adsorption rate ( $\text{mg g}^{-1} \text{min}^{-1}$ ) as  $t \rightarrow 0$ , and  $k_2$  is the rate constant ( $\text{g mg}^{-1} \text{min}^{-1}$ ) of pseudo-second-order adsorption.

These kinetic models will be discussed in detail in section 3.4.

### 1.8.2 Adsorption Isotherm

It is both fundamentally and commercially important to correlate equilibrium data between adsorbates and chitosan in order to assess chitosan's capacity for different adsorbates which ranged from dyes to metal ions and as a prerequisite for the design of commercial treatment system (Gerente et al., 2007). Besides, adsorption isotherm gives information on adsorption mechanisms, surface properties and affinity of an adsorbent towards the adsorbate (Ho et al., 2002).

In this study, three isotherm models were applied, which were Langmuir (Langmuir, 1916), Freundlich (Freundlich, 1906), and Dubinin-Radushkevich (Dubinin et al. 1947) isotherm models.

The linearized Langmuir equation is given as (Langmuir, 1916):

$$\frac{C_e}{q_e} = \frac{1}{Q_{\max} b} + \frac{C_e}{Q_{\max}} \quad (1.4)$$